

## Supplementary Material

# Determination of Zero-Field Splittings in $\text{Co}^{2+}$ Halides Complexes with Magnetic and Far-IR Measurements

Jia-Jia Liu,<sup>a</sup> Yin-Shan Meng,<sup>a</sup> Ivo Hlavička,<sup>b,c</sup> Milan Orlita,<sup>b</sup> Shang-Da Jiang,<sup>a,\*</sup> Bing-Wu Wang<sup>a</sup>,  
and Song Gao<sup>a,\*</sup>

<sup>a</sup> National Laboratory for Molecular Sciences, State Key Laboratory of Rare Earth Materials  
Chemistry and Applications, College of Chemistry and Molecular Engineering, Peking University,  
Beijing 100871 (P. R. China)

<sup>b</sup> Laboratoire National des Champs Magnétiques Intenses (LNCMI-EMFL), CNRS, UGA,  
38042 Grenoble, France

<sup>c</sup> CEITEC BUT, Brno University of Technology, 616 00 Brno, Czech Republic

Email: [jiangsd@pku.edu.cn](mailto:jiangsd@pku.edu.cn) and [gaosong@pku.edu.cn](mailto:gaosong@pku.edu.cn)

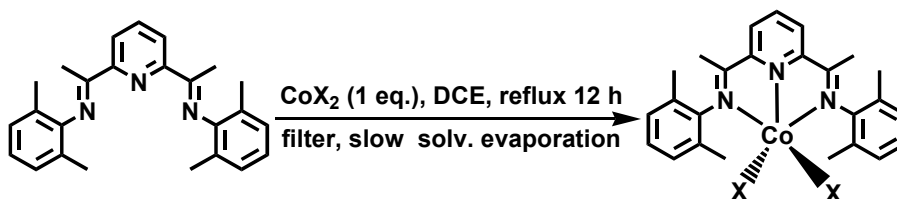
\*To whom correspondence should be addressed.

## EXPERIMENTAL SECTION

**General methods.** All manipulations and syntheses (without indication) described below were performed under air atmosphere. Unless otherwise noted, all starting materials were commercially available as reagent grade and were used without further purification.

**Preparation of 2,6-Bis[1-[(2,6-dimethylphenyl)imino]ethyl]pyridine (N<sub>3</sub>-Me).** 2,6-dimethylaniline (2.46 mL, 21.15 mmol) was added to a solution of 2,6-diacetylpyridine (1.08 g, 6.62 mmol) in absolute methanol (50 mL). After the addition of several drops of formic acid, the reaction mixture was refluxed for 24 h and then allowed to cool down to room temperature. The crude product precipitated as a yellow powder. Pure ligand was obtained (2.45 g for 92%) upon recrystallization from methanol.

Scheme S1. The synthesis route of complexes 1-3.



**Preparation of [Co(L)Cl<sub>2</sub>]DCE (CoCl).** A mixture of L (370 mg, 1 mmol) and CoCl<sub>2</sub>·6H<sub>2</sub>O (240 mg, 1 mmol) in dichloroethane (DCE) (100 mL) was refluxed for 12 h in the air and then allowed to cool down to room temperature. The resulting green solution was filtered and dark green block crystals suitable for X-ray diffraction were obtained within two weeks in 60-70 % yield by slow evaporation of the resulting solution. Anal. (%), CoCl, calcd. for C<sub>27</sub>Cl<sub>4</sub>N<sub>3</sub>CoH<sub>31</sub>: C, 54.20; H, 5.22; N, 7.02. Found: C, 54.29; H, 5.32; N, 7.12.

**Preparation of [Co(L)Br<sub>2</sub>]MeCN (CoBr) and [Co(L)I<sub>2</sub>]DCE (CoI).** Preparation of complexes CoBr and CoI is similar to that of CoCl except that the solvent for CoBr is acetonitrile (MeCN). CoBr,

calcd. for  $C_{27}Br_2N_4CoH_{30}$ : C, 51.53; H, 4.81; N, 8.90. Found: C, 51.62; H, 4.80; N, 8.94. CoI, calcd. for  $C_{27}I_2Cl_2N_3CoH_{31}$ : C, 41.51; H, 4.00; N, 5.38. Found: C, 41.64; H, 4.04; N, 5.49.

**Crystal structure determination.** The diffraction intensity data (SXR) for the single crystals of the three compounds at 180 K were collected on an Agilent Technology SuperNova Dual Atlas CCD diffractometer with a (Mo  $K\alpha$  = 0.71073 Å) microfocus source and focusing multilayer mirror optics. The determination of crystal class and unit cell parameters was carried out by the CrysAlisPro program. The raw frame data were processed using the CrysAlisPro program to yield the reflection data file. All structures were solved by direct method and refined by full-matrix least-squares on  $F^2$  using SHELXTL program. The analytical scattering factors for neutral atoms were used throughout the analysis. The hydrogen atoms were placed at the calculated positions and were included in the structure calculation without further refinement of the parameters. The details of data collection, data reduction and crystallographic data are summarized in Table S1-2.

The CCDC number 1536062-1536064 contain the supplementary crystallographic data for this paper. CIF files can be also downloaded free of charge at via [www.ccdc.cam.ac.uk/conts/retrieving.html](http://www.ccdc.cam.ac.uk/conts/retrieving.html) (or from the Cambridge Crystallographic Data Centre, 12 Union Road, Cambridge CB2 1EZ, UK; fax: (+44) 1223-336-033; or e-mail: [deposit@ccdc.cam.ac.uk](mailto:deposit@ccdc.cam.ac.uk)).

**Magnetic properties measurements.** Direct current (*dc*) magnetic measurements were performed on Quantum Design MPMSXL5 SQUID system with polycrystalline samples tightly packed and sealed in a capsule. Diamagnetic corrections were estimated using Pascal constants ( $299 \times 10^{-6} \text{ cm}^3 \text{ mol}^{-1}$ ,  $315 \times 10^{-6} \text{ cm}^3 \text{ mol}^{-1}$  and  $360 \times 10^{-6} \text{ cm}^3 \text{ mol}^{-1}$ ) and background correction by experimental

measurement on sample holders. Measurements of alternating current (*ac*) susceptibilities were carried out at a 3 Oe oscillating *ac* field below 10 K in the frequency range of 10 ~ 10000 Hz using Quantum Design PPMS-9T (EC-II) SQUID magnetometer.

**Magneto-transmission experiments.** Far-infrared magneto-transmission spectra were recorded on powder samples dispersed in eicosane in a ratio of 1:4, 1:4 and 1:6 for CoCl, CoBr and CoI, respectively. These mixed compounds were then pressed into pellets ~0.5 mm thick and put into sample holder on a Bruker IFS 66v/s FTIR spectrometer with a globar source, where the sample was placed inside an 11 T solenoid magnet, with a composite bolometer detector element located inside the magnet. All the spectra were recorded at 10K.  $T_B$  and  $T_0$  stand for transmission of the sample at zero and finite magnetic field B, respectively. The normalized experimental data are shown in the form of relative magneto-transmission  $T_B/T_0$ .

**Other physical properties measurements.** PXRD data for the four compounds were collected in the range of  $5^\circ < 2\theta < 50^\circ$  at room temperature for the bulk samples and the pressed tablet samples on a Rigaku Dmax 2000 diffractometer with Cu  $K\alpha$  radiation. Element analysis of carbon, nitrogen and hydrogen were performed on an Elementar Vario MICRO CUBE analyzer.

**Table S1** Crystallographic data for complex **CoCl**, **CoBr** and **CoI**, measured at 180 K

Compound	CoCl	CoBr	CoI
Formula	C <sub>27</sub> H <sub>31</sub> CoN <sub>3</sub> Cl <sub>4</sub>	C <sub>27</sub> H <sub>30</sub> CoN <sub>4</sub> Br <sub>2</sub>	C <sub>27</sub> H <sub>31</sub> CoN <sub>3</sub> I <sub>2</sub> Cl <sub>2</sub>
<i>T</i> , K	180	180	180
crystal system	monoclinic	monoclinic	triclinic
space group	<i>P</i> 2 <sub>1</sub> / <i>c</i>	<i>P</i> 2 <sub>1</sub> / <i>n</i>	<i>P</i> 2 <sub>1</sub> / <i>c</i>
<i>a</i> , Å	11.7147(4)	13.1235(15)	12.5631(6)
<i>b</i> , Å	15.0025(5)	14.7508(8)	18.9466(6)
<i>c</i> , Å	16.4202(5)	14.4264(10)	13.4530(5)
$\alpha$ , °	90	90	90
$\beta$ , °	99.118(3)	107.150(9)	109.094(5)
$\gamma$ , °	90	90	90
<i>V</i> , Å <sup>3</sup>	2849.38(15)	2668.5(4)	3026.0(2)
<i>Z</i>	4	4	4
<i>D</i> <sub>c</sub> , gcm <sup>-3</sup>	1.395	1.566	1.715
$\mu$ (Mo <i>K</i> $\alpha$ ), mm <sup>-1</sup>	0.998	3.660	2.800
<i>F</i> (000)	1236.0	1268.0	1524.0
Crystal size, mm <sup>3</sup>	0.3×0.16×0.06	0.31×0.22×0.15	0.22×0.15×0.14
<i>T</i> <sub>min</sub> , <i>T</i> <sub>max</sub>	0.684, 1.000	0.406, 0.711	0.679, 0.734
$\theta$ <sub>min</sub> , $\theta$ <sub>max</sub> , °	2.83, 26.02	2.96, 26.02	3.20, 26.02
no. total reflns.	15711	16564	19374
no. uniq. reflns ( <i>R</i> <sub>int</sub> )	5628(0.0277)	5251(0.0454)	5958(0.590)
no. obs. [ <i>I</i> ≥2σ( <i>I</i> )]	4660	3929	4596
no. params	322	308	322
<sup>a</sup> <i>R</i> 1, <sup>b</sup> <i>wR</i> 2 [ <i>I</i> ≥2σ( <i>I</i> )]	0.0346, 0.0770	0.0366, 0.0730	0.0350, 0.0738
<sup>a</sup> <i>R</i> 1, <sup>b</sup> <i>wR</i> 2 (all data)	0.0456, 0.0831	0.0606, 0.0809	0.0544, 0.0851
GOF	1.044	1.031	1.063
<sup>c</sup> $\Delta\rho$ , e/Å <sup>3</sup>	0.92, -0.83	0.60, -0.40	1.24, -1.11
<sup>d</sup> Max. and mean $\Delta/\sigma$	0.001, 0.000	0.001, 0.000	0.001, 0.000

*a.*  $R1 = \sum||F_o| - |F_c|| / \sum|F_o|$ ; *b.*  $wR2 = [\sum w(F_o^2 - F_c^2)^2 / \sum w(F_o^2)^2]^{1/2}$ ; *c.* Maximum and minimum residual electron density; *d.* Maximum and mean sigma/shift.

**Table S2** Selected bond distances (Å) and bond angles (°) of **CoCl**, **CoBr** and **CoI**.

<b>Compound</b>	<b>CoCl</b>	<b>CoBr</b>	<b>CoI</b>
Co-N1	2.0297(17)	2.022(2)	2.051(3)
Co-N2	2.2251(17)	2.251(3)	2.169(4)
Co-N3	2.2834(16)	2.264(3)	2.180(4)
Co-X1	2.2592(6)	2.3844(5)	2.5843(6)
Co-X2	2.2670(6)	2.4013(5)	2.6840(6)
N1-Co-N2	75.87(6)	75.90(11)	74.29(13)
N1-Co-N3	74.58(6)	74.97(11)	73.79(13)
N1-Co-X1	116.47(5)	116.88(7)	162.11(10)
N1-Co-X2	127.23(5)	128.21(7)	89.25(9)
N2-Co-N3	150.44(6)	150.73(9)	139.69(12)
N2-Co-X1	96.94(5)	96.58(6)	102.96(9)
N2-Co-X2	98.61(5)	99.20(7)	101.61(9)
N3-Co-X1	96.61(5)	98.96(6)	99.91(8)
N3-Co-X2	98.71(5)	96.52(6)	101.94(9)
X1-Co-X2	116.29(2)	114.90(2)	108.55(2)
CShM( $D_{3h}$ )	2.552	2.904	6.333
CShM( $C_{4v}$ )	4.023	3.889	3.253

**Table S3.** Summary of magnetic properties of compound **CoCl**, **CoBr** and **CoI**, listed  $\chi T$  values, zero-field splitting parameters and  $g$  factors were obtained by fitting  $dc$  susceptibility data, and effective energy barriers and relaxation times are obtained by fitting  $ac$  susceptibility data.

<b>Compound</b>	<b>CoCl</b>	<b>CoBr</b>	<b>CoI</b>
$(\chi T)_{300\text{ K}} / \text{cm}^3\text{Kmol}^{-1}$	2.90	2.98	2.95
$(M_{\text{sat}})_{2\text{ K}, 5\text{ T}} / \text{N}\beta$	2.18	2.25	2.24
${}^a D / \text{cm}^{-1}$	50(3)	40(2)	-26(1)
${}^a E / \text{cm}^{-1}$	10(1)	6(1)	7(1)
${}^b g$	2.45(1)	2.47(1)	2.52(1)
${}^c \text{Temp. Range} / \text{K}$	2.5-6.5	2.4-4.6	2.2-4.4
${}^d U_{\text{eff}} / \text{cm}^{-1}$	22(2)	16(1)	9(1)
${}^d \tau_0 / \text{s}$	$8.3 \times 10^{-7}$	$9.2 \times 10^{-7}$	$7.5 \times 10^{-6}$
${}^e U_{\text{theo}} / \text{cm}^{-1}$	106(5)	83(3)	57(3)
${}^f U_{\text{fir}} / \text{cm}^{-1}$	109(2)	90(2)	61(1)

*a.* Zero-field splitting parameters obtained from fitting the corresponding  $dc$  magnetic data with EasySpin program.

*b.*  $g$  factors derivate from fitting the corresponding  $dc$  magnetic data with EasySpin and Anisofit 2.0 program.

*c.* temperature range that the  $ac$  magnetic susceptibility shows frequency dependency.

*d.* effective energy barrier obtained by fitting the Arrhenius equation.

*e.* The calculation values obtained from the equation:  $U_{\text{theo}} = 2\sqrt{D^2 + 3E^2}$ .

**Figure S1** Crystal structure of  $\text{CoCl}$ . Packing diagram viewing from  $a$  (left),  $b$  (middle),  $c$  (right) directions, respectively. The red polyhedrons represent the local coordination structure of cobalt ions.

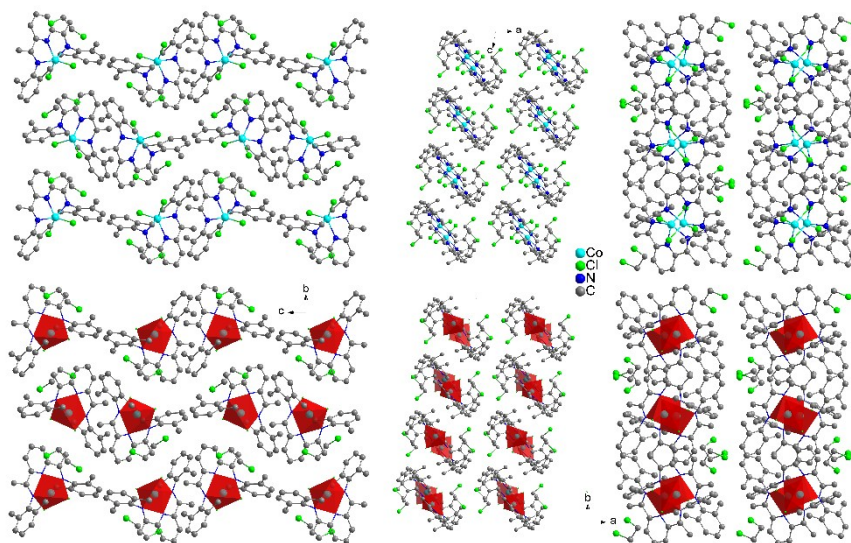




**Figure S2** Crystal structure of **CoBr**. Packing diagram viewing from *a* (left), *b* (middle), *c* (right) directions, respectively. The red polyhedrons represent the local coordination structure of cobalt ions.

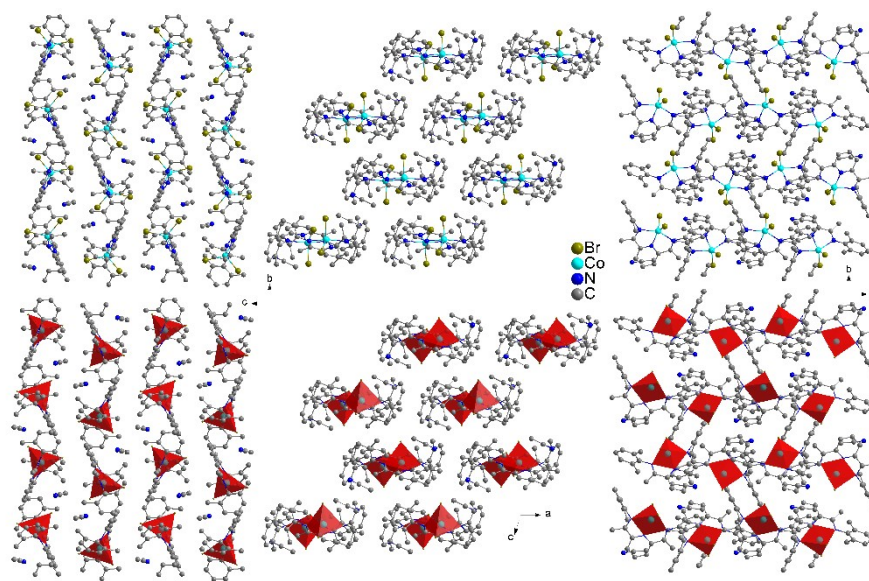


**Figure S3** Crystal structure of **CoI**. Packing diagram viewing from *a* (left), *b* (middle), *c* (right) directions, respectively. The red polyhedrons represent the local coordination structure of cobalt ions.

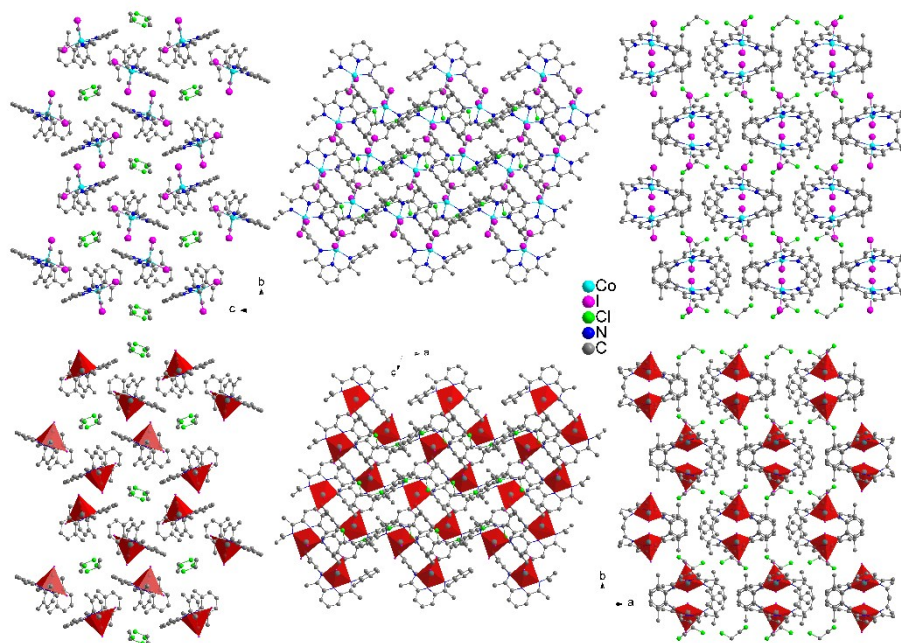


**Figure S4** PXRD patterns for as-prepared and pressed samples of **CoCl**, **CoBr** and **CoI**. The simulated one based on their single crystal structures at the temperature of 180 K.

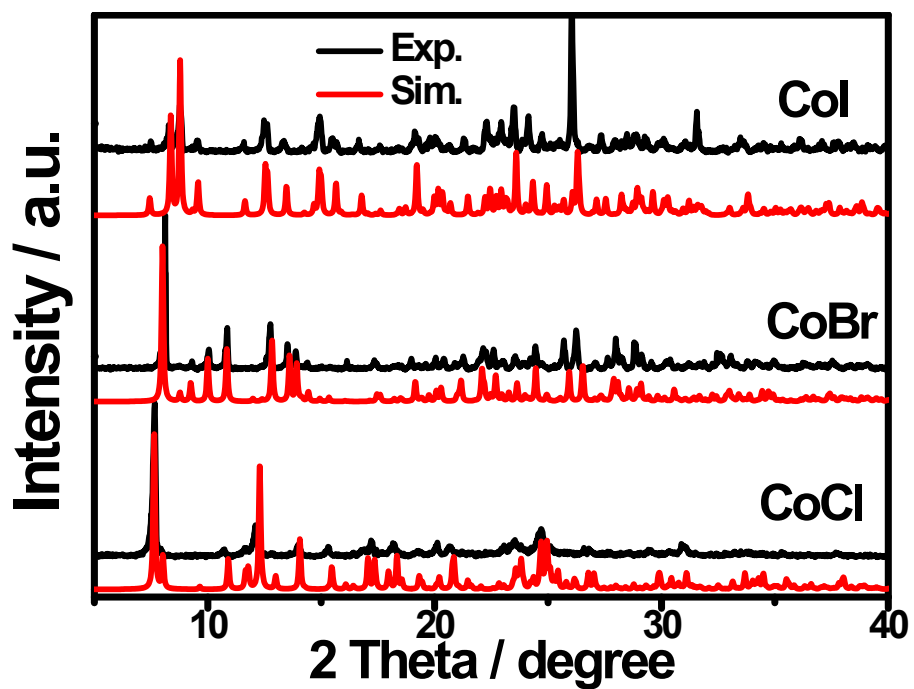


**Figure S5** (Up) Argand (Cole-Cole) plots for CoCl ( $H_{dc} = 1$  kOe,  $H_{ac} = 3$  Oe). Dots: experimental data. Black solid line: fitting result based on Debye Model. (Middle) Temperature dependence of in-phase ( $\chi'$ ) and out-of-phase magnetic susceptibility ( $\chi''$ ) of CoCl at various frequency under 1 kOe dc field. (Down) Plot of relaxation time ( $\ln \tau$ ) vs  $T^{-1}$  for CoCl.

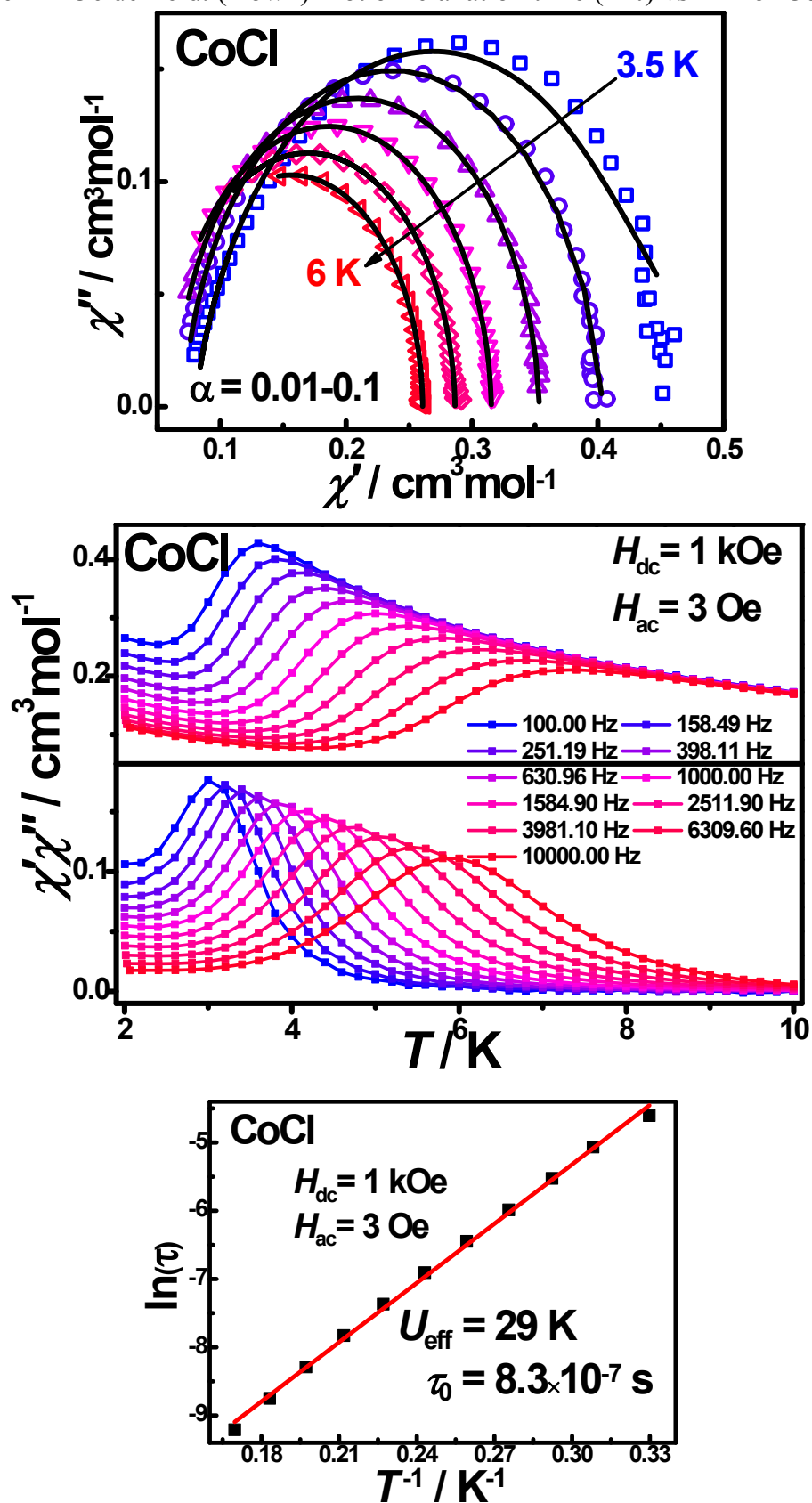




**Figure S6** (Up) Argand (Cole-Cole) plots for **CoBr** ( $H_{dc} = 2$  kOe,  $H_{ac} = 3$  Oe). Dots: experimental data. Black solid line: fitting result based on Debye Model. (Middle) Temperature dependence of in-phase ( $\chi'$ ) and out-of-phase magnetic susceptibility ( $\chi''$ ) of CoBr at various frequency under 2 kOe dc field. (Down) Plot of relaxation time ( $\ln \tau$ ) vs  $T^{-1}$  for CoBr.

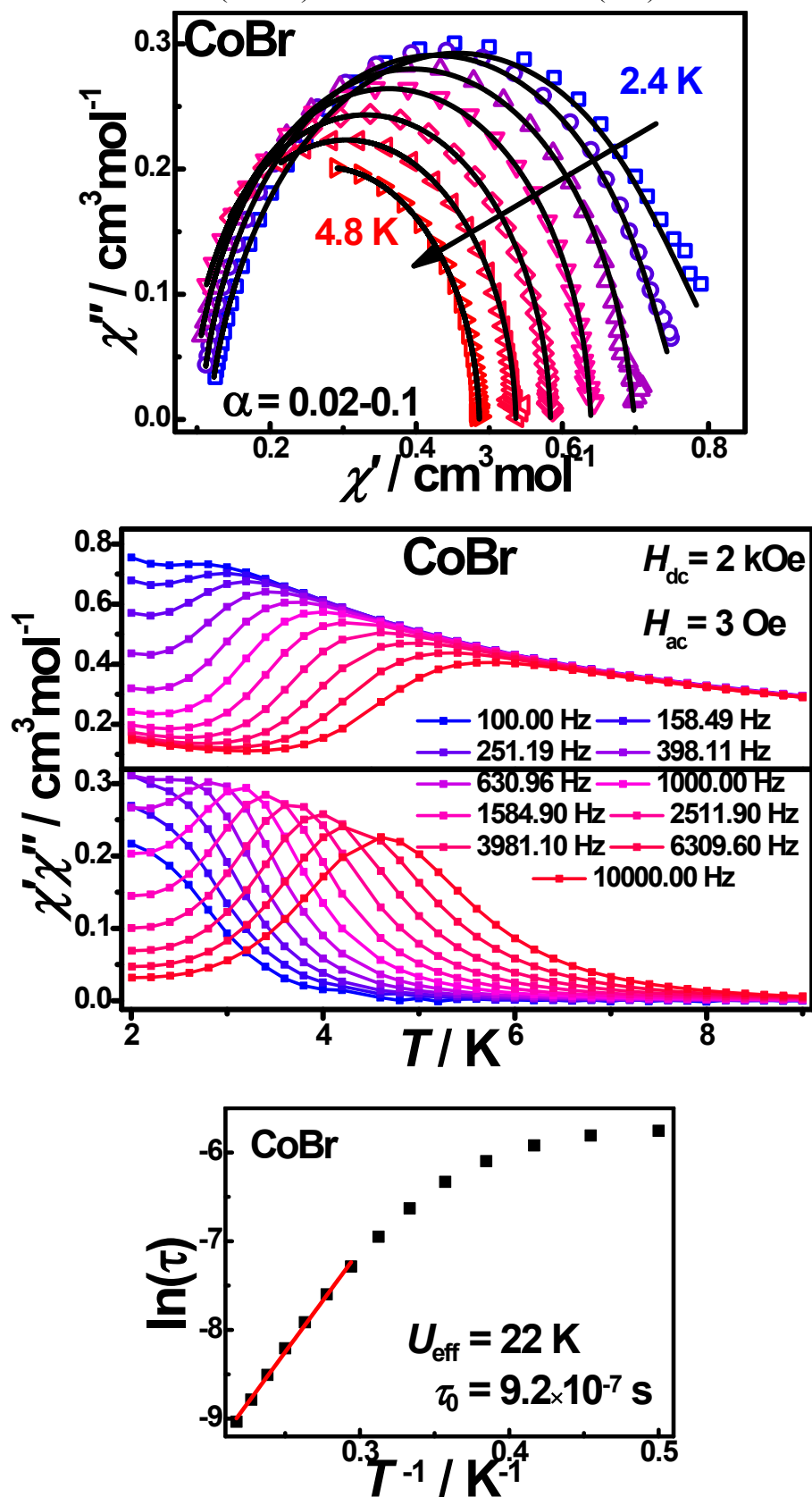




**Figure S7** (Up) Argand (Cole-Cole) plots for CoI ( $H_{dc} = 2$  kOe,  $H_{ac} = 3$  Oe). Dots: experimental data. Black solid line: fitting result based on Debye Model. (Middle) Temperature dependence of in-phase ( $\chi'$ ) and out-of-phase magnetic susceptibility ( $\chi''$ ) of CoI at various frequency under 2 kOe dc field. (Down) Plot of relaxation time ( $\ln \tau$ ) vs  $T^{-1}$  for CoI.

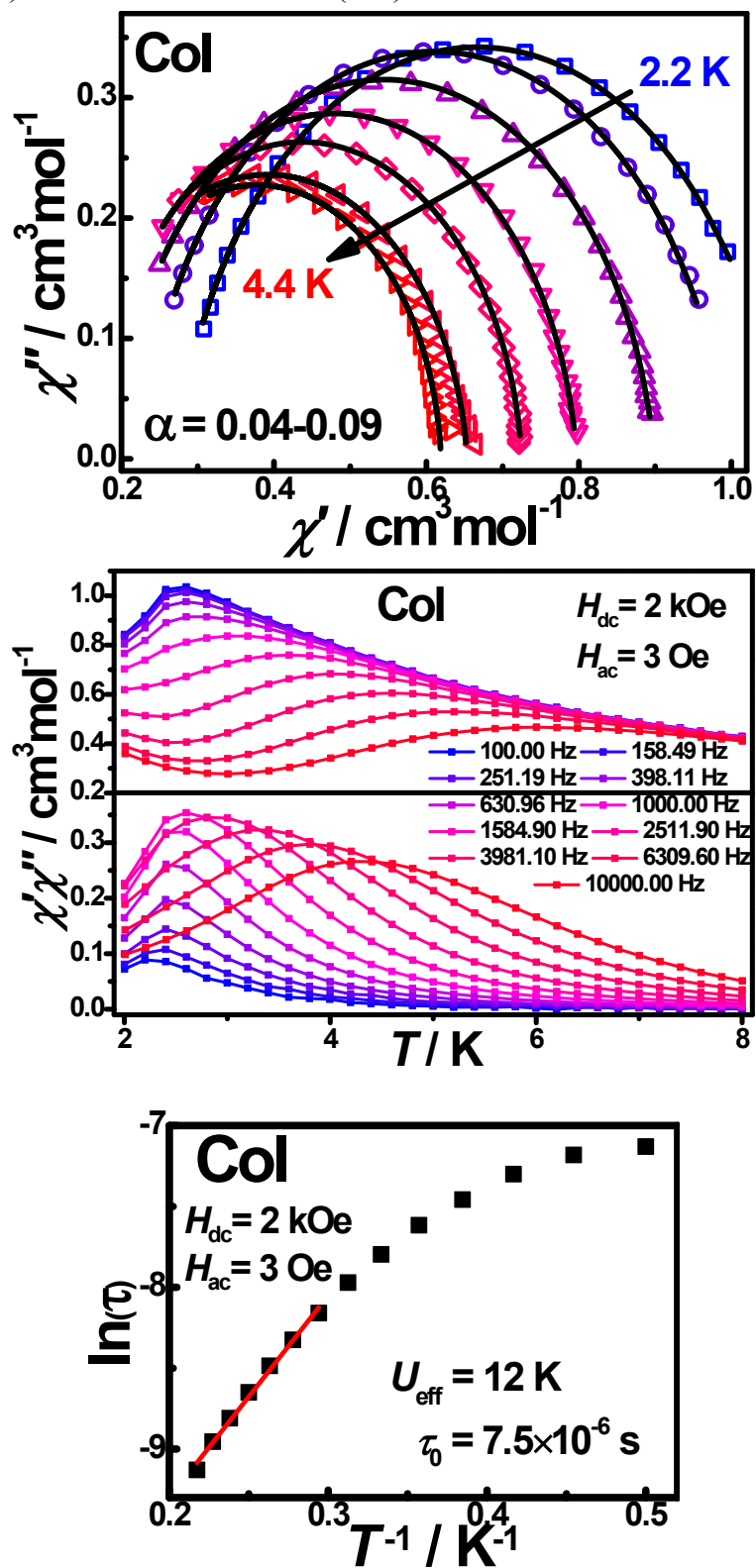




**Figure S8** Magneto-transmission spectra of **CoCl** in the field of 0 - 11 T.

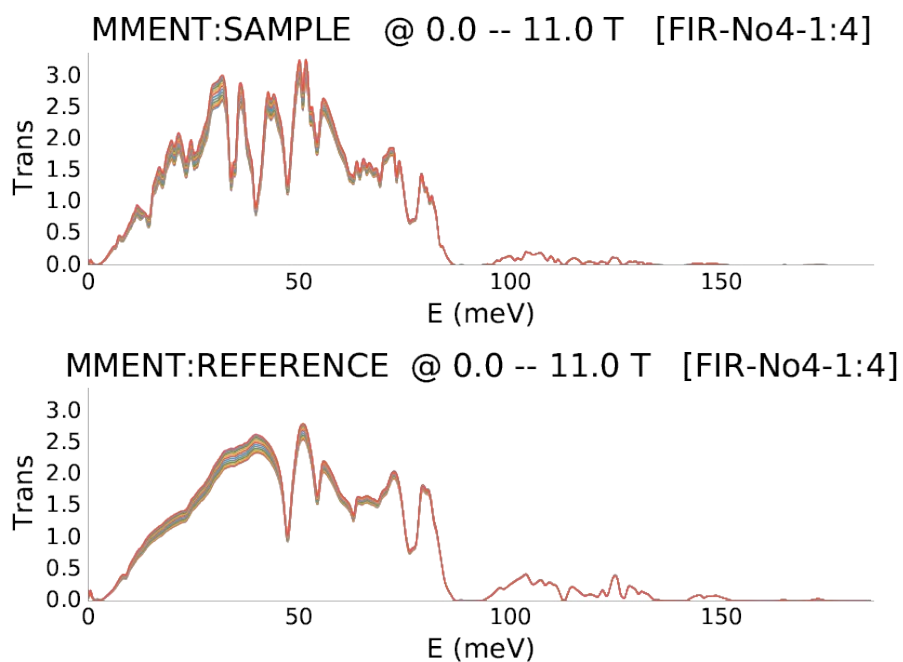


**Figure S9** magneto-transmission spectra of **CoBr** in the field of 0 - 11 T

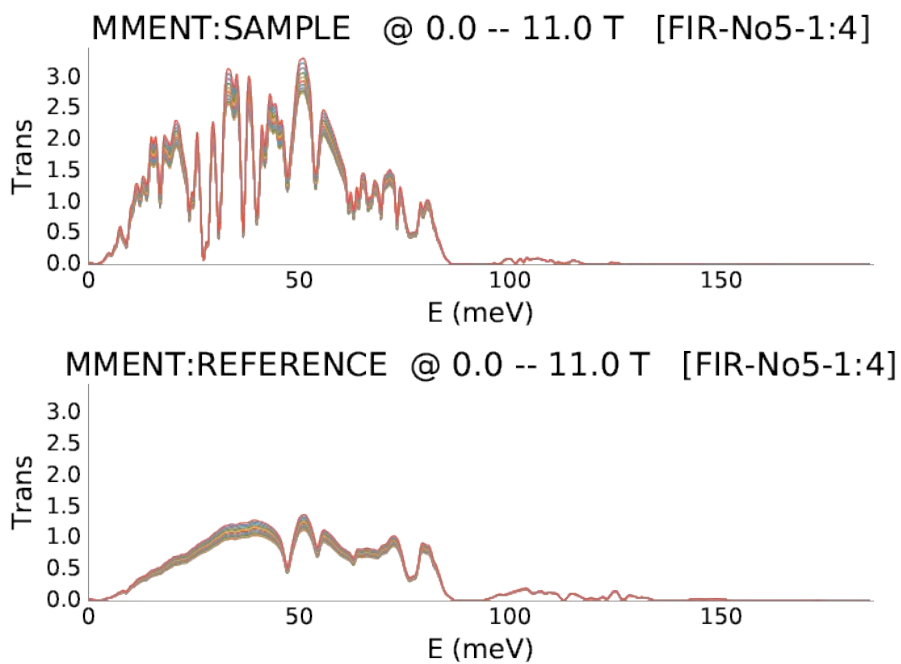


**Figure S10** magneto-transmission spectra of **CoI** in the field of 0 - 11 T.

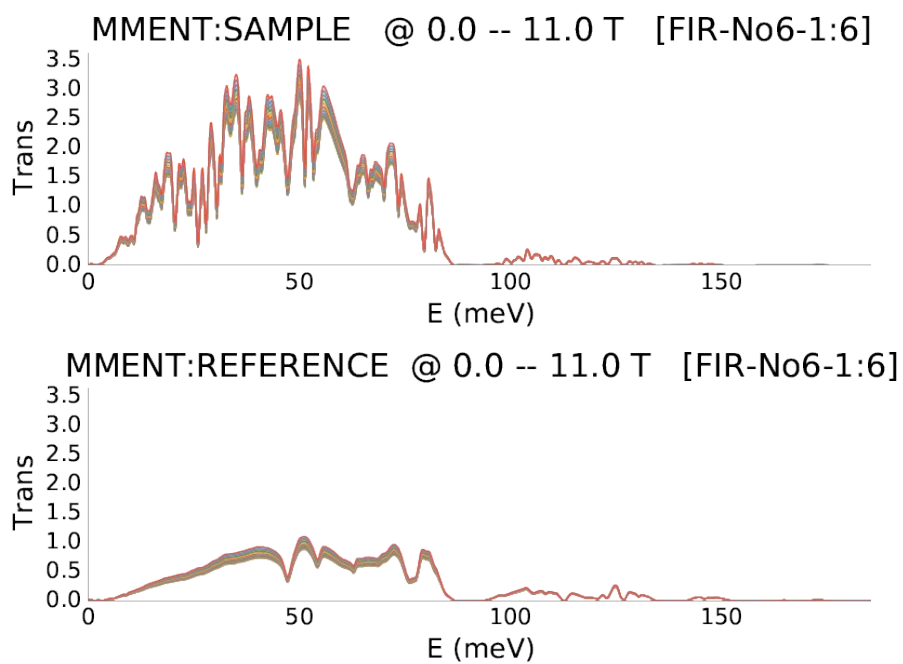


**Figure S11** magneto-transmission spectra of (a) **CoCl**, (b) **CoBr** and (c) **CoI** at  $B = 0-11$  T in the form of  $T_s/T_r$  (denote as  $T_B$  and  $T_0$  in the main text) in the range of  $50 - 200$   $\text{cm}^{-1}$ .

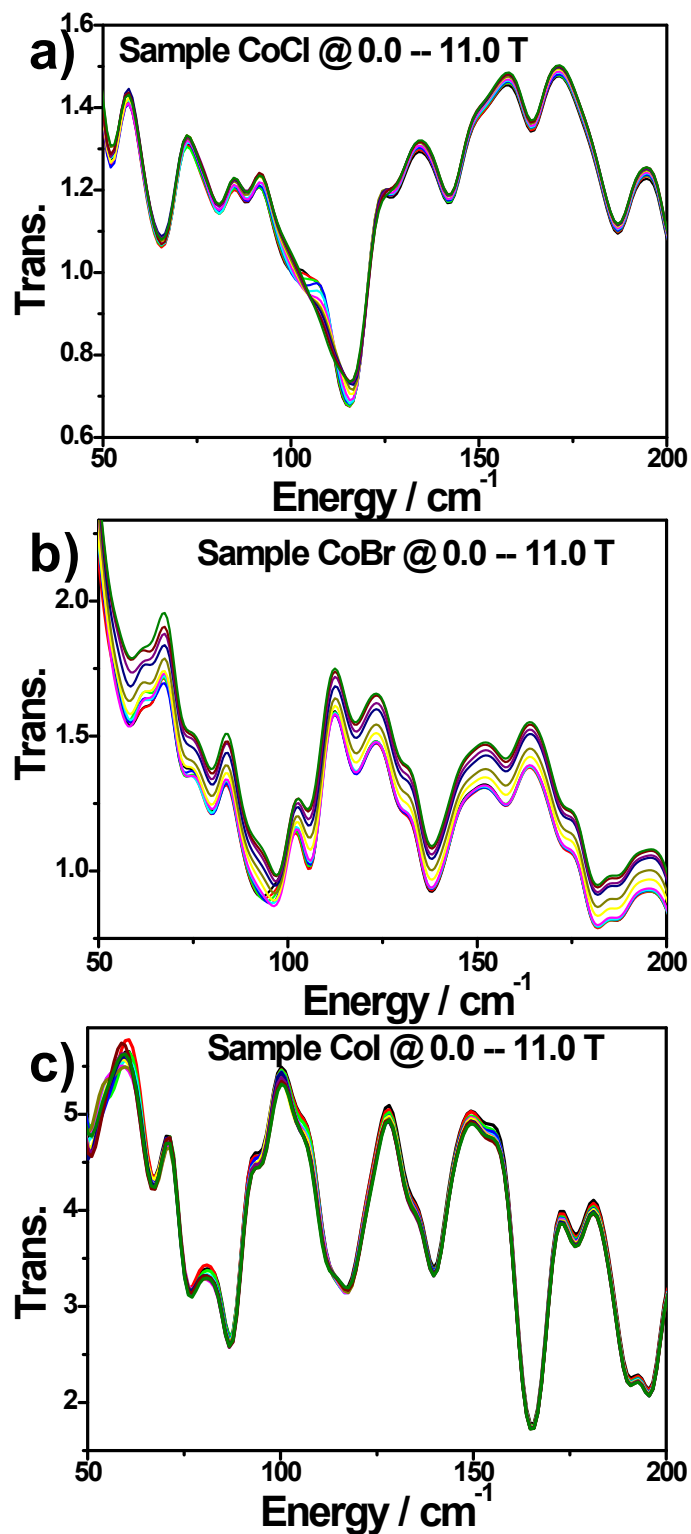


**Figure S12** Normalized magneto-transmission spectra of (a) **CoCl**, (b) **CoBr** and (c) **CoI**. The experimental data are shown in the form of relative magneto-transmission  $T_B/T_0$ .

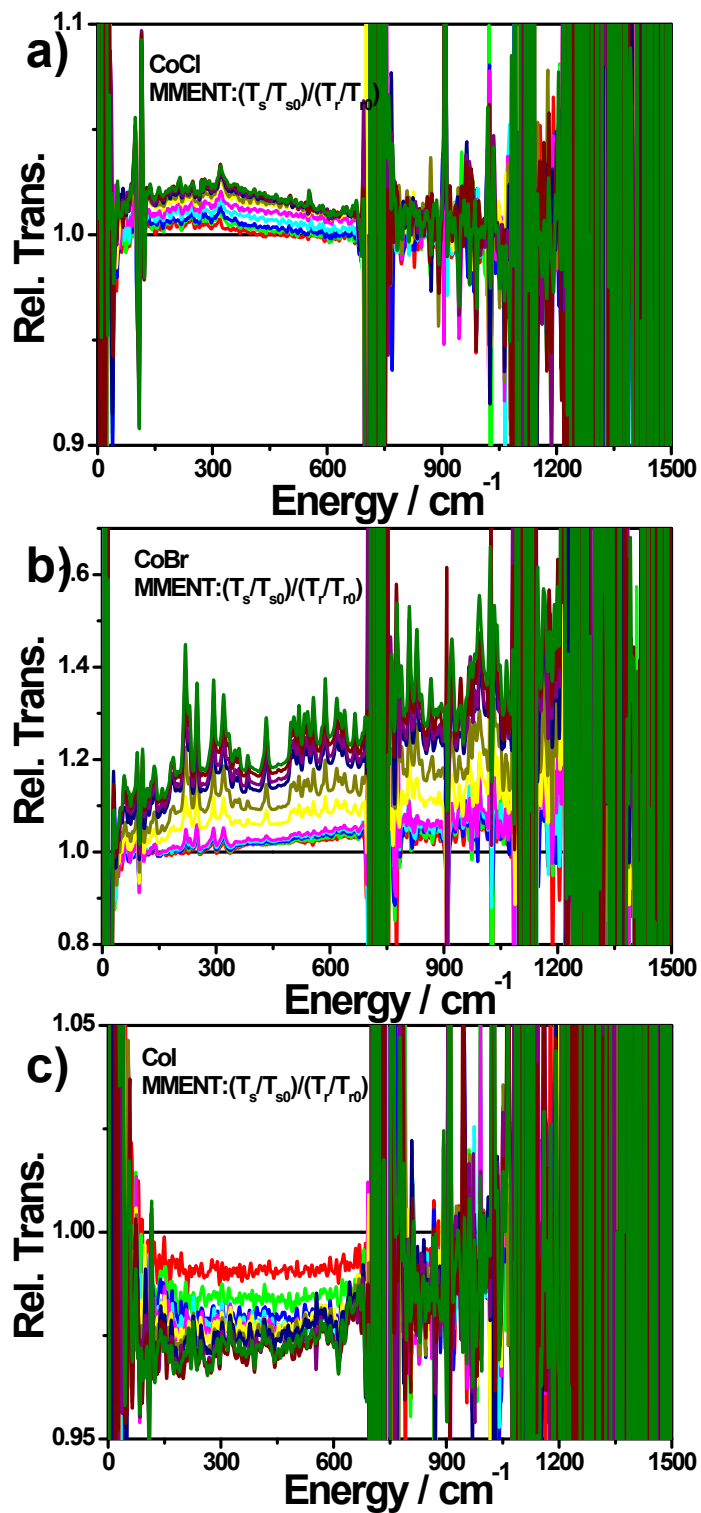


**Figure S13** field optimization measurements of compounds **1** (a), **2** (b) and **3** (c) at different fields (0-4000 Oe) and different temperatures.

